

Original Paper

Mammalian STE20-Like Kinase 1 Deletion Alleviates Renal Ischaemia-Reperfusion Injury via Modulating Mitophagy and the AMPK-YAP Signalling Pathway

Junxia Feng Hongyan Li Yunfang Zhang Qi Wang Shili Zhao
Ping Meng Jingchun Li

Department of Nephrology, Huadu District People's Hospital of Guangzhou, Southern Medical University, Guangzhou, China

Key Words

Renal ischaemia-reperfusion injury • Mitophagy • Apoptosis • OPA1 • AMPK-YAP signalling pathway

Abstract

Background/Aims: The aim of our study is to investigate the molecular mechanism by which mammalian STE20-like kinase 1 (Mst1) participates in renal I/R injury through modifying mitophagy and the AMPK-YAP signalling pathway. **Methods:** WT mice and Mst1-knockout mice were subjected to renal ischaemia-reperfusion (I/R) *in vivo*. *In vitro*, the hypoxia-reoxygenation model was used with renal tubular epithelial cells to mimic renal I/R injury. Mitochondrial function was monitored via western blotting and immunofluorescence. Pathway blocker and siRNA knockout technology were used to establish the role of the AMPK-YAP signalling pathway in Mst1-mediated mitochondrial apoptosis in the setting of renal I/R injury. **Results:** Our data demonstrated that Mst1 expression was upregulated in response to renal I/R injury *in vivo*, and a higher Mst1 content was positively associated with renal dysfunction and more tubular epithelial cell apoptosis. However, genetic ablation of Mst1 improved renal function, alleviated reperfusion-mediated tubular epithelial cell apoptosis, and attenuated the vulnerability of kidney to I/R injury. *In vitro*, Mst1 upregulation induced mitochondrial damage including mitochondrial potential reduction, ROS overloading, cyt-c liberation and caspase-9 apoptotic pathway activation. At the molecular levels, I/R-mediated mitochondrial damage via repressing mitophagy and Mst1 suppressed mitophagy via inactivating AMPK signalling pathway and downregulating OPA1 expression. Re-activation of AMPK-YAP-OPA1 signalling pathway provided a survival advantage for the tubular epithelial cell in the context of renal I/R injury by repressing mitochondrial fission. **Conclusion:** Overall, our results demonstrate that the pathogenesis of renal I/R injury is closely associated with an increase in Mst1 expression

and the inactive AMPK-YAP-OPA1 signalling pathway. Based on this, strategies to repress Mst1 expression and activate mitophagy could serve as therapeutic targets to treat kidney ischaemia-reperfusion injury.

© 2018 The Author(s)
Published by S. Karger AG, Basel

Introduction

Revascularization via reperfusion therapy is the standard modality for patients with ischemic renal damage [1]. Unfortunately, although reperfusion restores blood flow to infarcted kidney tissues, the reperfusion itself also induces additional damage to the kidney tissue, which is referred to as ischemia-reperfusion (I/R) injury [2, 3]. In spite of the extensive research that has been carried out over the past six decades in the field of renal IR injury [4, 5], the pathogenesis of reperfusion-mediated kidney damage is poorly understood [6].

Mitochondria are the center of cell energy production and the triggers of programmed cell death [7, 8]. Normal mitochondria produce ATP to fuel cellular metabolism through oxidative phosphorylation [9]. However, damaged mitochondria liberate the proapoptotic factors, such as cytochrome c, into the cytoplasm, thereby initiating caspase-9-related programmed cell death [10]. Numerous studies have identified mitochondria as potential targets to regulate the progression of renal IR injury [11-16]. However, the role of mitophagy in renal I/R injury has not been appropriately investigated. Mitophagy, a kind of mitochondrial autophagy, is a highly regulated process involving the degradation of damaged mitochondria with the assistance of lysosomes in mammalian cells. Moderate mitophagy has been acknowledged as a protective mechanism, accounting for cell metabolism, proliferation and survival [17]. Mitophagy activation is accompanied by a decline in the mass of poorly structured mitochondria and is also reported to be involved in mitochondrial biosynthesis [18]. The functional role of mitophagy has been explored in acute cardiac I/R injury [19] and chronic liver fatty disease [20]. Increased mitophagy enhances the resistance of cardiomyocytes against reperfusion stress and retards hepatocyte stenosis and apoptosis in the setting of a high-fat diet [21-22]. However, the exact role of mitophagy in renal IR injury remains controversial.

Mammalian STE20-like kinase 1 (Mst1), also known as serine/threonine-protein kinase 4, is the downstream effector of the Hippo signalling pathway. Several studies have suggested the causal relationship between Mst1 upregulation and cell death. Mst1 activation promotes hepatoma cell death via the PHLPPA-Akt signalling pathway [23]. Brain ischaemia-reperfusion injury and neuronal apoptosis are also related to Mst1 activation [24, 25]. Mst1 also participates in atherosclerosis progression via autophagy inhibition and macrophage apoptosis [26]. Many researchers have attempted to demonstrate the promotive effects of Mst1 on acute cell death. However, no study has investigated the contribution of Mst1 to renal I/R injury. Moreover, Mst1 has been reported to be associated with mitochondrial damage in myocardial ischaemia reperfusion injury [27], pancreatic cancer cells [28], and spinal cord trauma [29]. This evidence supports the possibility that Mst1 can be considered the upstream regulator of mitochondrial homeostasis during acute cell stress. However, whether Mst1 can regulate mitophagy is incompletely understood.

Materials and Methods

Renal I/R injury model in vivo and in vitro

The procedure of the I/R injury model was performed as previously described [30]. In short, I/R injury was achieved by unilateral clamping (micro aneurysm clamps) in one renal pedicle for 30 min under general inhalation anaesthesia (3% isoflurane and oxygen). Reperfusion was induced via removal of the clamps for approximately 4 hours. Sham-operated mice underwent the same procedure except for clamping of the renal pedicles [31]. The renal tubular epithelial cell line LLC-PK1, purchased from the American Type Culture Collection (ATCC® CL-101™) was cultured in DMEM medium (Gibco/Thermo Fisher, Waltham, MA,

USA) supplemented with 10% FBS (Gibco/Thermo Fisher, Waltham, MA, USA) in a humidified incubator at 37°C and 5% CO₂. When the cells reached 70%-80% confluence, they were treated with the hypoxia-reoxygenation (H/R) model *in vitro*. The H/R model was achieved via 30 minutes of hypoxia and 4 hours of reoxygenation. Hypoxia preconditioning was performed using cells cultured in a tri-gas incubator with the N₂ concentration at 95% and CO₂ concentration at 5% for approximately 30 min. Next, reoxygenation injury was induced for 4 h in cells under normal culture conditions [32]. To observe the functional role of Mst1 in H/R-mediated cell apoptosis, siRNA against Mst1 and their negative controls were transfected into cells to repress Mst1 expression. In addition, a pathway blocker of AMPK was used to prevent AMPK activation. Briefly, Compound C (CC, 10 μM, Selleck Chemicals, Houston, TX, USA) was added to the cell medium for 45 minutes to inhibit the AMPK activation.

Cell death detection

MTT was used to analyze the cellular viability. LLC-PK1 cells (1x10⁶ cells/well) were cultured on a 96-well plate at 37°C with 5% CO₂. Then, 40 μl of MTT solution (2 mg/ml; Sigma-Aldrich) was added to the medium for 4 h at 37°C with 5% CO₂. Subsequently, the cell medium was discarded, and 80 μl of DMSO was added to the wells for 1 h at 37°C with 5% CO₂ in the dark. The OD of each well was observed at 490 nm via a spectrophotometer (Epoch 2; BioTek Instruments, Inc., Winooski, VT, USA). The LDH release assay was performed according to the manufacturer's instructions [33].

Apoptotic cells were also detected with an In Situ Cell Death Detection Kit (Thermo Fisher Scientific Inc., Waltham, MA, USA; Catalog No. C1024) according to the manufacturer's protocol [34]. Briefly, cells were fixed with 4% paraformaldehyde at 37°C for 15 min. Blocking buffer was added to the wells, and then cells were permeabilized with 0.1% Triton X-100 in 0.1% sodium citrate for 2 min on ice. The cells were incubated with TUNEL reaction mixture for 1 h at 37°C. DAPI (Sigma-Aldrich, St. Louis, MO, USA) was used to counterstain the nuclei, and the numbers of TUNEL-positive cells were recorded. Five fields per section and three sections per kidney were examined in each experimental group.

ATP detection

Cellular ATP generation was measured to reflect mitochondrial function. First, cells were washed with cold PBS three times at room temperature. Then, a luciferase-based ATP assay kit (Celltiter-Glo Luminescent Cell Viability assay; Promega, Madison, WI, USA; Catalog No. A22066) was used to analyze the ATP content according to the instructions [35]. ATP production was measured via a microplate reader (Epoch 2; BioTek Instruments, Inc.).

siRNA transfection and knockdown assay

Cells were seeded in 6-well clusters and then were incubated at 37°C in 5% CO₂ until 80% confluent. Mst1 siRNA was purchased from Santa Cruz, USA. siRNA transfection solution was prepared according to the directions provided by Santa Cruz to make a siRNA solution at a concentration of 400 nM [36]. The cells were washed once with siRNA transfection medium (Santa Cruz, USA). Next, appropriate siRNA transfection medium and siRNA transfection solution were added to each well. The cells were then incubated for 6 hours at 37°C in 5% CO₂. The transfection mixture was then removed and replaced with normal growth medium, and then the cells were incubated for an additional 24 hours. Western blotting was performed to observe the knockdown efficiency [37].

Immunofluorescence

The cells were washed twice with PBS, permeabilized in 0.1% Triton X-100 overnight at 4°C. After the fixation procedure, the sections were cryoprotected in a PBS solution supplemented with 0.9 mol/l of sucrose overnight at 4°C. After neutralization with NH₄Cl buffer, the sections were permeabilized for 45 min with 0.05% saponin/PBS (pH=7.4) and incubated overnight with the following primary antibodies [38]: p-CREB (1:1000, Cell Signaling Technology, #9198), Mfn2 (1:1,000, Abcam, #ab56889), Tom20 (1:1,000, Abcam, #ab186735), LAMP1 (1:1000, Abcam, #ab24170), cyt-c (1:1000; Abcam; #ab90529) [39].

ELISA

Glutathione (GSH, Thermo Fisher Scientific Inc., Waltham, MA, USA; Catalog No. T10095), glutathione peroxidase (GPX, Beyotime Institute of Biotechnology, China; Catalog No. S0056) and SOD (Thermo Fisher Scientific Inc., Waltham, MA, USA; Catalog No. BMS222TEN) were measured according to the manufacturer's instructions using a microplate reader (Epoch 2; BioTek Instruments, Inc.) [40]. To analyze changes in caspase-9, caspase-9 activity kits (Beyotime Institute of Biotechnology, China; Catalog No. C1158) were used according to the manufacturer's protocol. In brief, to measure caspase-9 activity, 5 μ l of LEHD-p-NA substrate (4 mM, 200 μ M final concentration) was added to the samples for 1 hour at 37°C. Then, the absorbance at 400 nm was recorded via a microplate reader to reflect the caspase-3 and caspase-9 activities. To analyze caspase-3 activity, 5 μ l of DEVD-p-NA substrate (4 mM, 200 μ M final concentration) was added to the samples for 2 hours at 37°C.

Measurement of reactive oxygen species (ROS) and mitochondrial membrane potential

ROS production was analyzed via flow cytometry according to a previous study. Cells were washed with cold PBS and cultured with an ROS probe (1 mg/ml, DHE, Molecular Probes, USA) at 37°C in the dark for 15 minutes. After the cells were washed with cold PBS three times, the cells were collected using 0.25% pancreatin. After resuspension in cold PBS, the cells were analyzed using a flow cytometer (BD FACSVerser; BD Biosciences, San Jose, CA, USA). To observe the mitochondrial potential, JC-1 staining (Thermo Fisher Scientific Inc., Waltham, MA, USA; Catalog No. M34152) was used. Then, 10 mg/ml JC-1 was added to the medium for 10 minutes at 37°C in the dark to label the mitochondria. Normal mitochondrial potential showed red fluorescence, and damaged mitochondrial potential showed green fluorescence [41].

Western blotting

After treatment, the infarcted kidneys were collected and washed with ice-cold PBS and lysed with RIPA buffer, and the total protein concentration was measured using the BCA assay (Nanjing Keygen Biotech Co., Ltd., Nanjing, Jiangsu, China). The lysates (50-70 μ g) were separated by 10% SDS-polyacrylamide gel (10-15%) electrophoresis (SDS-PAGE) [42]. Proteins were electrotransferred onto the Pure Nitrocellulose Blotting membrane (Life Sciences) (Millipore, Bedford, MA, USA) and then blocked with 5% nonfat milk for 2 hr at room temperature. The membrane was washed with TBST and then incubated with primary antibody: pro-caspase-3 (1:1000, Cell Signaling Technology, #9662), cleaved caspase-3 (1:1000, Cell Signaling Technology, #9664), Bax Monoclonal Antibody (6A7) (1:1000, Thermo Fisher Scientific, #14-6997-81), Bcl2 (1:1000, Cell Signaling Technology, #3498), caspase-9 (1:1000, Abcam #ab32539), LC3II (1:1000, Cell Signaling Technology, #3868), LC3I (1:1000, Cell Signaling Technology, #4599), Atg5 (1:1000, Cell Signaling Technology, #12994), p-ERK (1:1000, Abcam, #ab176660), t-ERK (1:1000, Abcam #ab54230), cyt-c (1:1000; Abcam; #ab90529), c-IAP (1:1000, Cell Signaling Technology, #4952), t-CREB (1:1000, Cell Signaling Technology, #9197), p-CREB (1:1000, Cell Signaling Technology, #9198), NR4A1 (1:1000, Cell Signaling Technology, #3960), Tom20 (1:1, 000, Abcam, #ab186735). The second antibodies used in the present study were as follows: Horseradish peroxidase-conjugated secondary antibodies (1:2, 000; cat. nos. 7076 and 7074; Cell Signaling Technology, Inc.). Band intensities were normalized to the respective internal standard signal intensity (GAPDH (1:1000, Cell Signaling Technology, #5174) and/or β -actin (1:1000, Cell Signaling Technology, #4970) using Quantity One Software (version 4.6.2; Bio-Rad Laboratories, Inc.) [43].

Statistical analyses

All experiments were repeated at least 3 times for each group, and the data are presented as the means \pm SEM. The data were analysed by ANOVA, followed by Fisher's least significant difference test, using SPSS software, version 13.0 (SPSS, Chicago, IL, USA).

Results

Mst1 is upregulated by renal I/R stress and promotes kidney damage

To verify the role of Mst1 in renal I/R injury, a 30-minute ischemia and 4-hour reperfusion model was established. After I/R injury, the kidney tissues were collected, and the alterations in Mst1 were measured. Compared to the sham group, I/R injury clearly increased the transcription (Fig. 1A) and expression (Fig. 1B-C) of Mst1. To understand whether increased Mst1 participates in renal I/R injury, Mst1 knockout (Mst1-KO) mice were used. Compared to the sham group, I/R injury drastically upregulated proapoptotic proteins, such as Bax, Bad and caspase-3 (Fig. 1D-I). In contrast, the content of antiapoptotic proteins, such as Bcl2 and c-IAP, were unfortunately downregulated in response to I/R stress (Fig. 1D-I). Interestingly, Mst1 deletion subtly reversed the concentrations of antiapoptotic factors and prevented the activation of proapoptotic mediators (Fig. 1D-I), suggesting that I/R injury evoked kidney cell death by upregulating Mst1. In agreement with the increase in caspase-3 expression, the protein activity of caspase-3 was also elevated in I/R-treated kidneys and was reduced to near-normal levels with Mst1 deletion (Fig. 1J).

Consistent with the *in vivo* observations, the LLC-PK1 cells undergoing hypoxia-reoxygenation (HR) injury also demonstrated decreased cell viability (Fig. 1K) and increased cell death (Fig. 1L-M), as assessed by the LDH-release assay and TUNEL staining, respectively. Subsequently, Mst1 siRNA and control siRNA was transfected into cells and the transfection was determined via western blotting. After being transfected with Mst1 siRNA, the viability of HR-treated LLC-PK1 cells was significantly increased (Fig. 1K-M), and the cell death ratio was markedly reduced (Fig. 1K-M). Altogether, these results indicate that Mst1 is primarily upregulated by renal I/R injury, and higher Mst1 coincides with significant damage to the perfused kidney by promoting cell death.

Mst1 deficiency attenuates reperfusion-mediated mitochondrial damage

Mitochondria are cellular organelles that are pivotal for regulation of renal cell death and survival during reperfusion burden [44-45]. Based on this, subsequent experiments were performed to analyze mitochondrial function. First, the cellular ATP concentration was measured to reflect mitochondrial metabolism. Compared to the control group, HR injury significantly reduced ATP generation (Fig. 2A), the effect of which was reversed by Mst1 knockdown. At the molecular level, cellular ATP is derived from the mitochondrial membrane potential; the mitochondrial respiratory complex converts the electric potential energy into ATP chemical energy. Interestingly, the mitochondrial potential was reduced with HR stress, as evidenced by a reduced red/green fluorescence ratio measured by the JC-1 kits (Fig. 2B-C). However, loss of Mst1 stabilized the mitochondrial potential (Fig. 2B-C). These results indicate that reperfusion injury promotes mitochondrial potential collapse, which causes the cellular ATP shortage.

The mitochondrial potential reduction is an early feature of mitochondrial apoptosis [46]. Loss of mitochondrial potential promotes electron leakage into the cytoplasm, producing superfluous ROS, which triggers mitochondrial membrane oxidation and the opening of mPTP. As shown in Fig. 2D-E, the flow cytometry analysis of mitochondrial ROS demonstrated that IR significantly increased ROS production, and this effect was negated by Mst1 deletion. In response to ROS overproduction, the mPTP opening rate was largely elevated in HR-treated cells and was considerably reduced to the near-normal levels with Mst1 knockdown (Fig. 2F).

The mPTP opening would facilitate the mitochondrial proapoptotic factor leakage into the cytoplasm, activating caspase-related programmed cellular death [47]. We performed an immunofluorescence assay to observe the mitochondrial proapoptotic factor liberation. As shown in Fig. 2G, mitochondrial cytochrome c was substantially released into the nucleus under HR challenge, and this tendency was effectively repressed by Mst1 deletion. This finding was further supported by western blotting which illustrated that Mst1 deletion largely downregulated the content of cytoplasmic cytochrome c and reversed the expression of mitochondrial

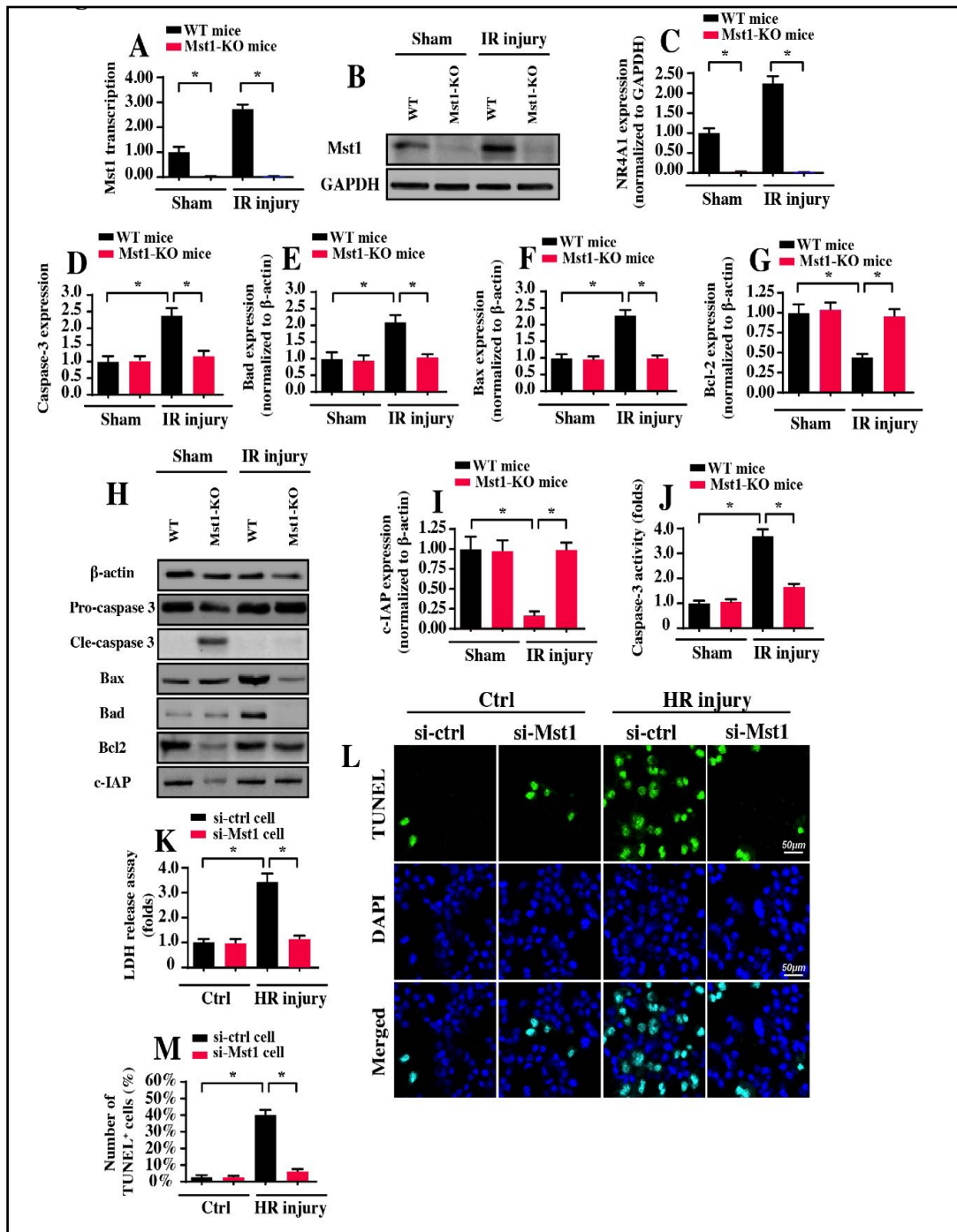
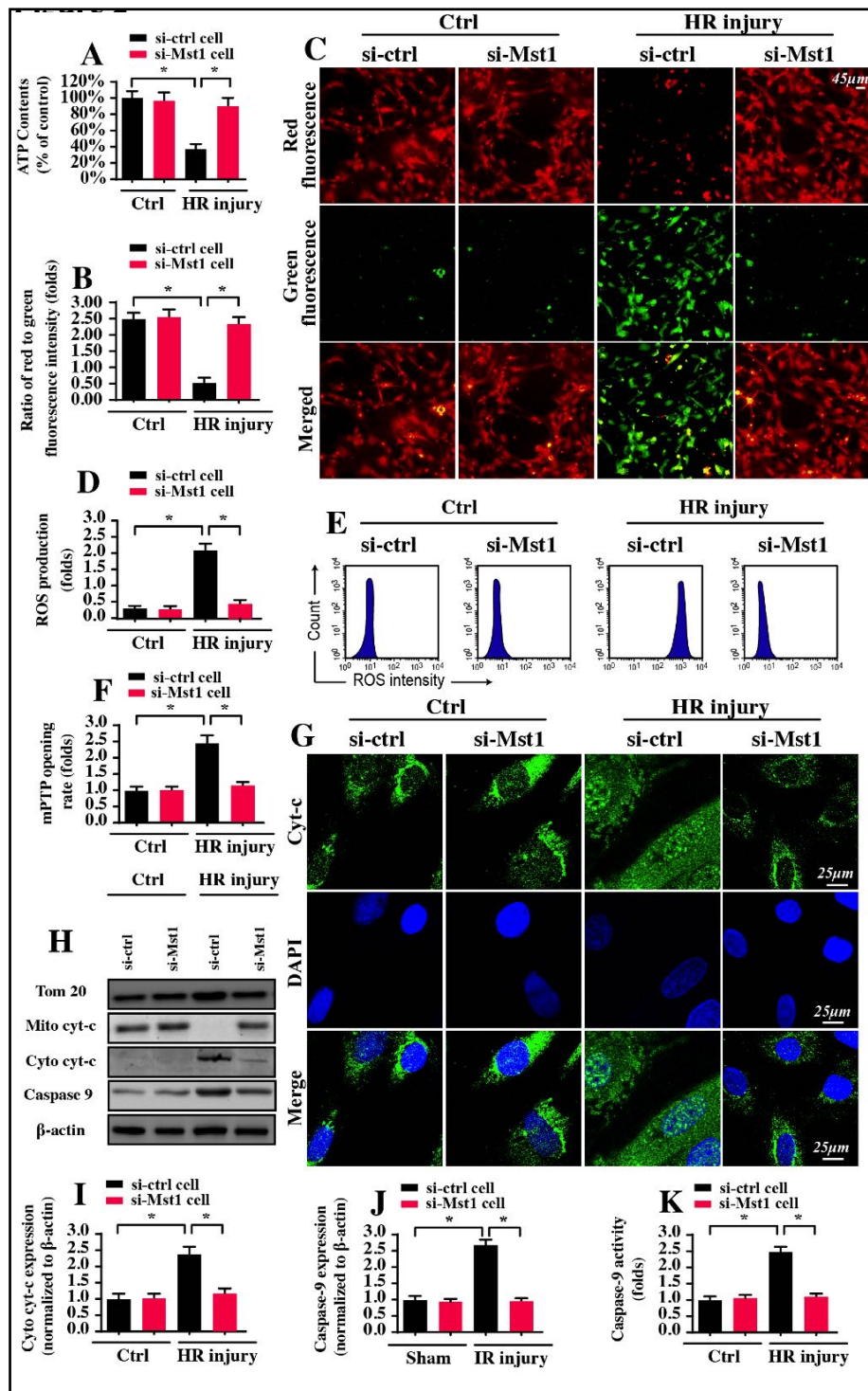


Fig. 1. Increased Mst1 promotes I/R-mediated renal damage. A. Wild-type (WT) mice and Mst1 knockout (Mst1-KO) mice were subjected to renal IR injury. Then, the kidney tissues were isolated, and qPCR was performed to analyze the alterations in Mst1 expression. B-C. Proteins were isolated in reperfused kidneys, and the expression of Mst1 was monitored. D-I. After renal IR injury, the kidney tissues were collected, and western blotting analysis was conducted to estimate the alterations in apoptosis-related factors. J. The tissues in reperfused kidneys were collected, and caspase-3 activity was evaluated to reflect cell death. K. In vitro, LLC-PK1 cells were used with a hypoxia reoxygenation (HR) model to mimic the animal renal IR injury. Mst1 siRNA was transfected into the LLC-PK1 cells to inhibit Mst1 expression in response to IR injury. Then, the cellular viability was determined via an LDH assay. L-M. Cell death was observed via an TUNEL staining. * $P < 0.05$.

Fig. 2. Mst1 deletion reduces mitochondrial apoptosis. A. Cellular ATP production was measured using an ATP detection kit. Mst1 siRNA was transfected into cells to inhibit Mst1 expression in response to HR injury. HR injury caused a drop in ATP generation, and this effect was reversed by Mst1 deletion. B-C. Mitochondrial potential was detected via JC-1 staining. The ratio of red to green fluorescence intensity was used to quantify the mitochondrial potential. D-E. Cellular ROS was evaluated using a DHE probe and was analyzed via flow cytometry. F. The mPTP opening rate was measured



using tetramethylrhodamine ethyl ester. G. Immunofluorescence assay for cyt-c. DAPI was used to stain the nucleus. The relative expression of nuclear cyt-c was monitored. H-J. After HR injury in vitro, the protein was isolated, and western blotting was performed to analyze the expression of cyt-c and caspase-9. K. Caspase-9 activity was determined via ELISA. *P<0.05.

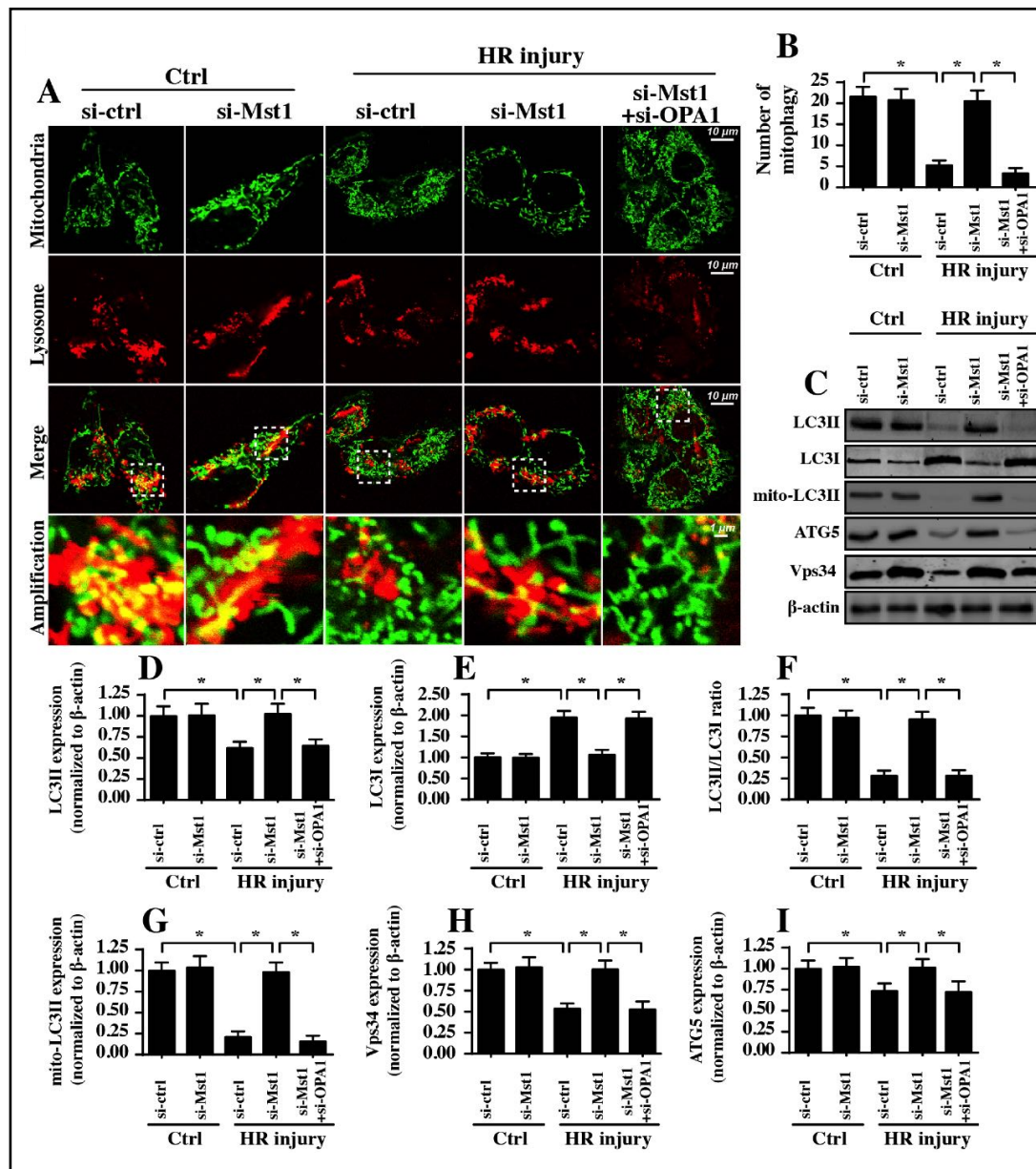


Fig. 3. Mst1 regulates OPA1-related mitophagy under HR injury. A. Mitophagic activity was measured by observing the fusion between mitochondria and lysosomes with the help of immunofluorescence. Mst1 siRNA and OPA1 siRNA were transfected into cells to inhibit Mst1 and OPA1 expression, respectively. B. The red mitochondrial fusion with green lysosomes generated the orange mitophagy, and the amount of mitophagy was recorded. C-I. After HR injury *in vitro*, the proteins were isolated, and western blotting was performed to analyze the alterations in proteins related to mitophagy. Mst1 siRNA and OPA1 siRNA were transfected into cells to inhibit Mst1 and OPA1 expression, respectively. *P<0.05.

cyt-c (Fig. 2H-I). Moreover, we also found that the expression (Fig. 2J) and activity (Fig. 2K) of caspase-9, the molecular characteristics of mitochondrial apoptosis, were both increased in response to HR stress, suggesting the activation of caspase-9-dependent mitochondrial apoptosis. However, Mst1 knockdown notably repressed caspase-9 activation (Fig. 2H-K). Altogether, our data demonstrate that Mst1 deletion strongly abrogated HR-initiated mitochondrial apoptosis *in vitro*.

Mst1 deficiency reverses OPA1-mediated mitophagy

In response to mitochondrial damage, mitophagy could remove the poorly structured mitochondria in a timely manner with the help of lysosomes, adequately sustaining mitochondrial homeostasis. Given this, we explored the alterations in mitophagy in response to renal I/R injury. First, the immunofluorescence assay was performed to observe the mitophagy by costaining mitochondria and lysosomes (Fig. 3A-B). Compared to the control group, HR treatment unfortunately disrupted the cooperation between mitochondria and lysosomes, as evidenced by decreased fusion of the mitochondria and lysosomes (Fig. 3A-B). Interestingly, Mst1 deletion capably promoted the interaction between mitochondria and lysosomes, suggesting mitophagic activation with Mst1 deletion. These results indicate that mitophagy is strongly inhibited by HR injury and is robustly reactivated by Mst1 deletion. Subsequently, mitophagic parameters were measured via western blotting according to a previous study. As shown in Fig. 3C-I, the LC3II expression was reduced and the content of LC3I was increased in response to HR injury. In addition, we further isolated the mitochondria and analyzed the expression of mitochondrial LC3II (mito-LC3II). The results shown in Fig. 3C-I indicated that the levels of mito-LC3II were also downregulated in the HR-treated group compared to those in the control group. Moreover, other mitochondrial autophagic markers, such as ATG5 and Vps34, were also repressed by HR stress. Interestingly, loss of Mst1 reversed the expression of mito-LC3II, ATG5 and Vps34, reconfirming the permissive effect of Mst1 deletion on mitophagy.

To verify whether OPA1 was necessary for mitophagy activation, siRNA against OPA1 was transfected into Mst1-deleted cells. Then, the mitophagic parameters were measured again. As shown in Fig. 3C-I, HR-inhibited mitophagy could be vastly reversed by Mst1 deletion, and this effect was nullified by OPA1 knockdown, as evidenced by decreased expression of mito-LC3II, ATG5 and Vps34. Altogether, these results indicate that Mst1 could sustain mitophagy by upregulating OPA1 under HR stress.

OPA1-related mitophagy ameliorates IR-initiated mitochondrial damage

To explain whether mitophagy sends a protective signal to the damaged mitochondria in the presence of HR injury, we evaluated mitochondrial function again. First, HR-repressed ATP production was significantly reversed by Mst1 deletion, and the beneficial effects of Mst1 deletion were invalidated by OPA1 knockdown (Fig. 4A). Similarly, the concentration of cellular antioxidant factors, such as GSH, GPX and SOD (Fig. 4B-D), were downregulated in response to HR stress and were reversed to near-normal levels with Mst1 deletion. However, loss of OPA1 abrogated the promotive effects of Mst1 deletion on antioxidants, suggesting that Mst1 regulates cellular redox balance via OPA1-related mitophagy.

Moreover, the HR-induced cyt-c leakage into the nucleus was strongly inhibited by Mst1 deletion (Fig. 4E-F); this effect was dependent on OPA1 because OPA1 knockdown re-evoked cyt-c translocation to the nucleus. Finally, the activity of caspase-9 (Fig. 4G), the hallmark of mitochondrial apoptosis, was increased by HR injury and was reduced to near-normal levels with Mst1 deletion in an OPA1-dependent manner. Altogether, the above data confirm that Mst1 handles mitochondrial homeostasis via OPA1-related mitophagy in the setting of renal HR injury.

Mst1 controls OPA1-related mitophagy via the AMPK-YAP signaling pathways

Next, experiments were conducted to analyze the upstream regulator of mitophagy. Previous studies have reported that AMPK-YAP is a classical signaling pathway responsible for mitophagy activation in different disease models [45]. Based on this, we asked whether the AMPK-YAP axis was required for OPA1-related mitophagy in an HR setting. Compared to the control group, HR injury significantly repressed the expression of p-AMPK, an effect that was accompanied by a drop in YAP (Fig. 5A-C), suggesting that the AMPK-YAP pathways were inactivated by HR injury. Interestingly, loss of Mst1 could reverse the content of p-AMPK and YAP (Fig. 5A-C), indicating the activation of the AMPK-YAP cascade with Mst1 deletion. Next, to verify whether the AMPK-YAP axis is necessary for OPA1 regulation under HR

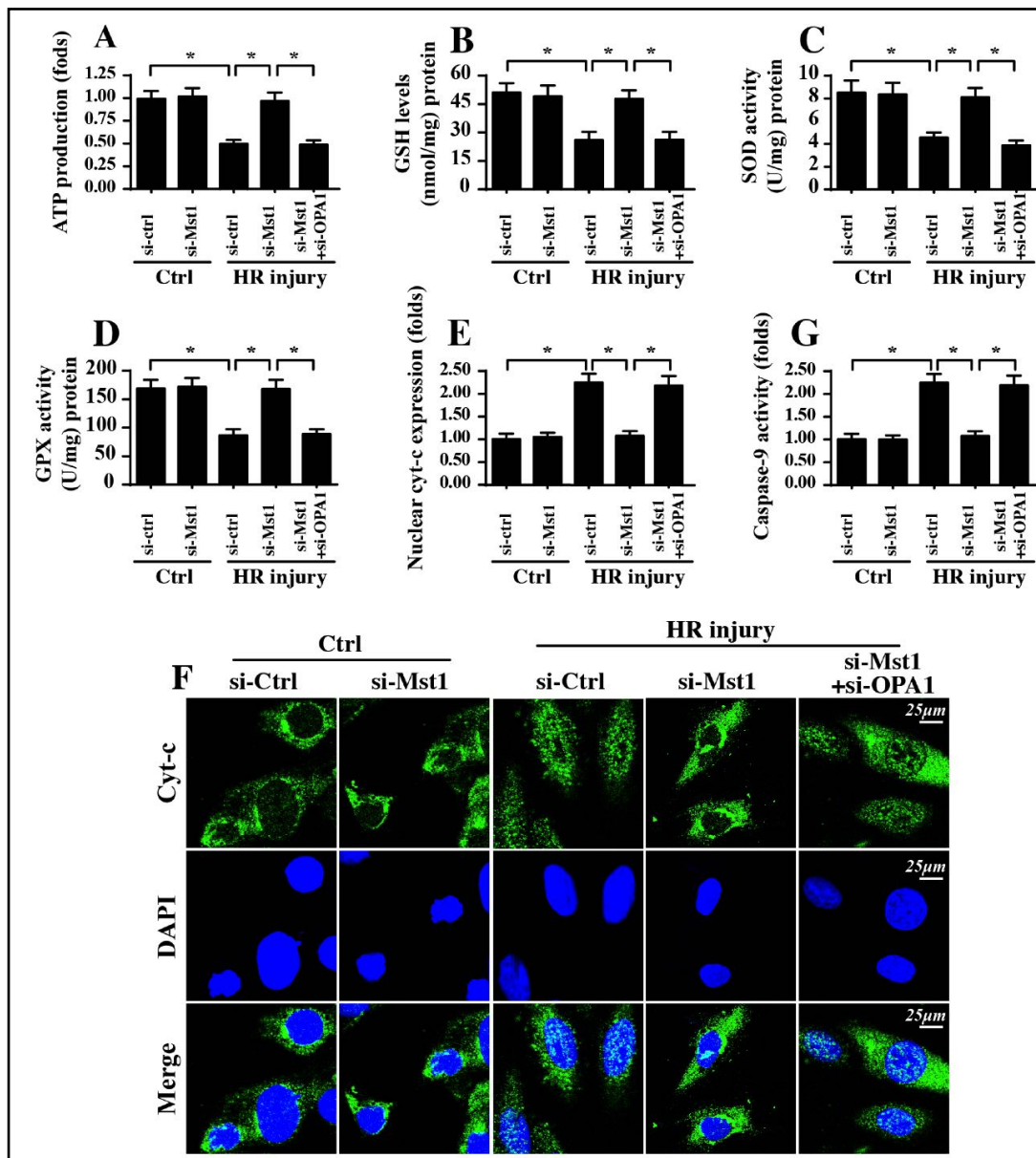
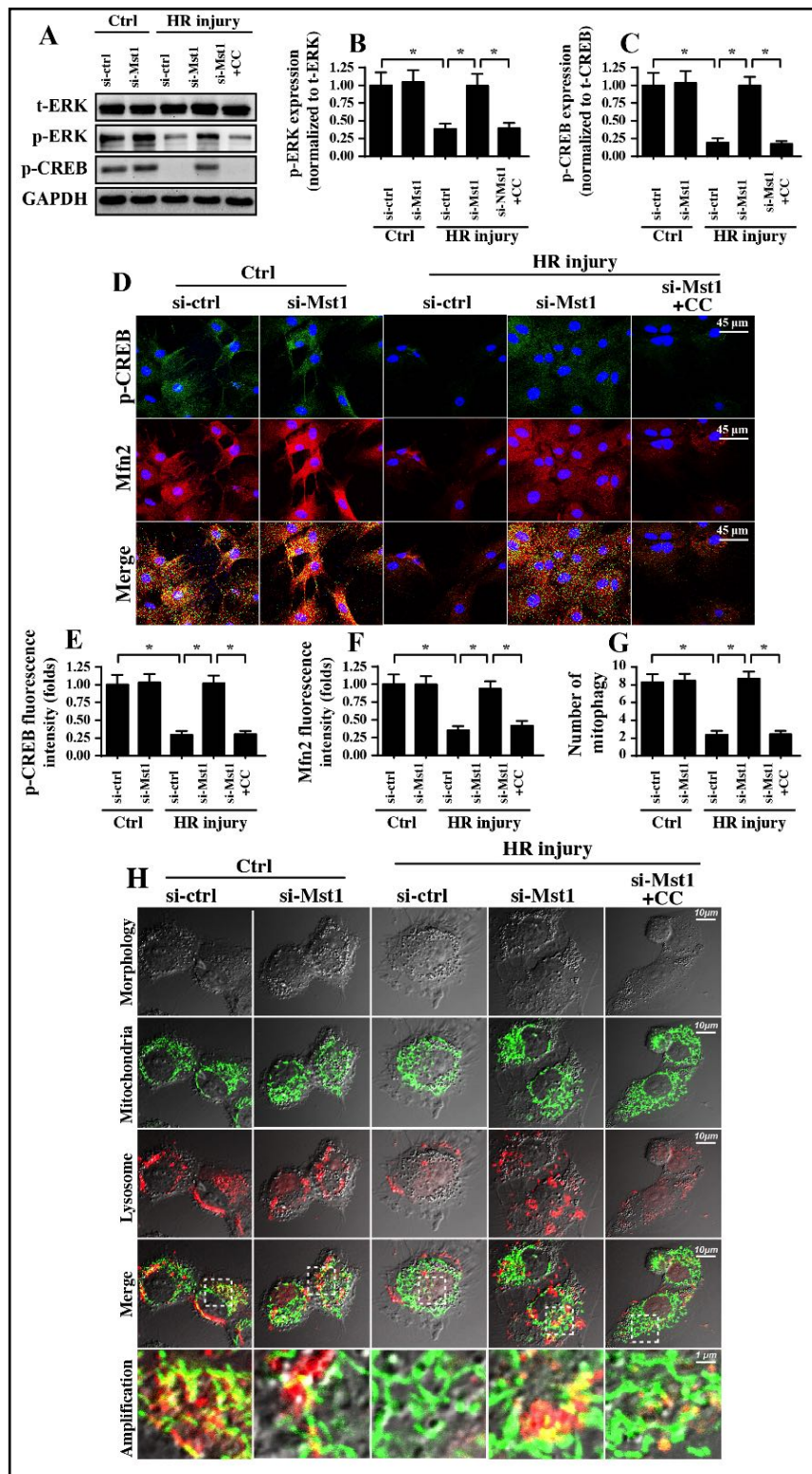


Fig. 4. OPA1-related mitophagy attenuates HR-mediated mitochondrial damage. A. ATP production was measured via an ATP detection kit. Mst1 siRNA and OPA1 siRNA were transfected into the cells to inhibit Mst1 and OPA1 expression, respectively. B-D. The concentration of cellular antioxidants was measured via ELISA. E-F. Immunofluorescence assay for cyt-c. DAPI was used to stain the nucleus. The relative expression of nuclear cyt-c was monitored. Mst1 siRNA and OPA1 siRNA were transfected into cells to inhibit Mst1 and OPA1 expression, respectively. G. Caspase-9 activity was evaluated via ELISA, and the relative caspase-9 activity was recorded as the ratio to the control group. Mst1 siRNA and OPA1 siRNA were transfected into cells to inhibit Mst1 and OPA1 expression, respectively. *P<0.05.

injury, a pathway blocker was added to the Mst1-deleted cells. After inhibition of AMPK, YAP expression was downregulated, an effect that was followed by reductions in the expression of OPA1 (Fig. 5D-F), as assessed by immunofluorescence.

To this end, to answer whether the AMPK-YAP axis is responsible for Mst1-modified mitophagy under HR injury, immunofluorescence for mitophagy was performed again. Compared to the control group, HR interrupted the fusion between mitochondria and lysosomes, indicating mitophagic inhibition (Fig. 5G-H). In contrast, Mst1 deletion largely

Fig. 5. Mst1 regulates OPA1-related mitophagy via AMPK-YAP pathways. A-C. Western blotting was performed to analyze the activation of the AMPK-YAP pathways with HR treatment. Mst1 siRNA was transfected into the cells to inhibit Mst1 expression. To inhibit the AMPK pathway, Compound C (CC) pretreatment was conducted for 2 hours. D-F. Immunofluorescence assay for p-AMPK and OPA1. G-H. Mitophagy was evaluated via an immunofluorescence assay. The amount of mitophagy was recorded. Mst1 siRNA was transfected into cells to inhibit Mst1 expression. CC was used to inhibit the AMPK-YAP pathways. *P<0.05.



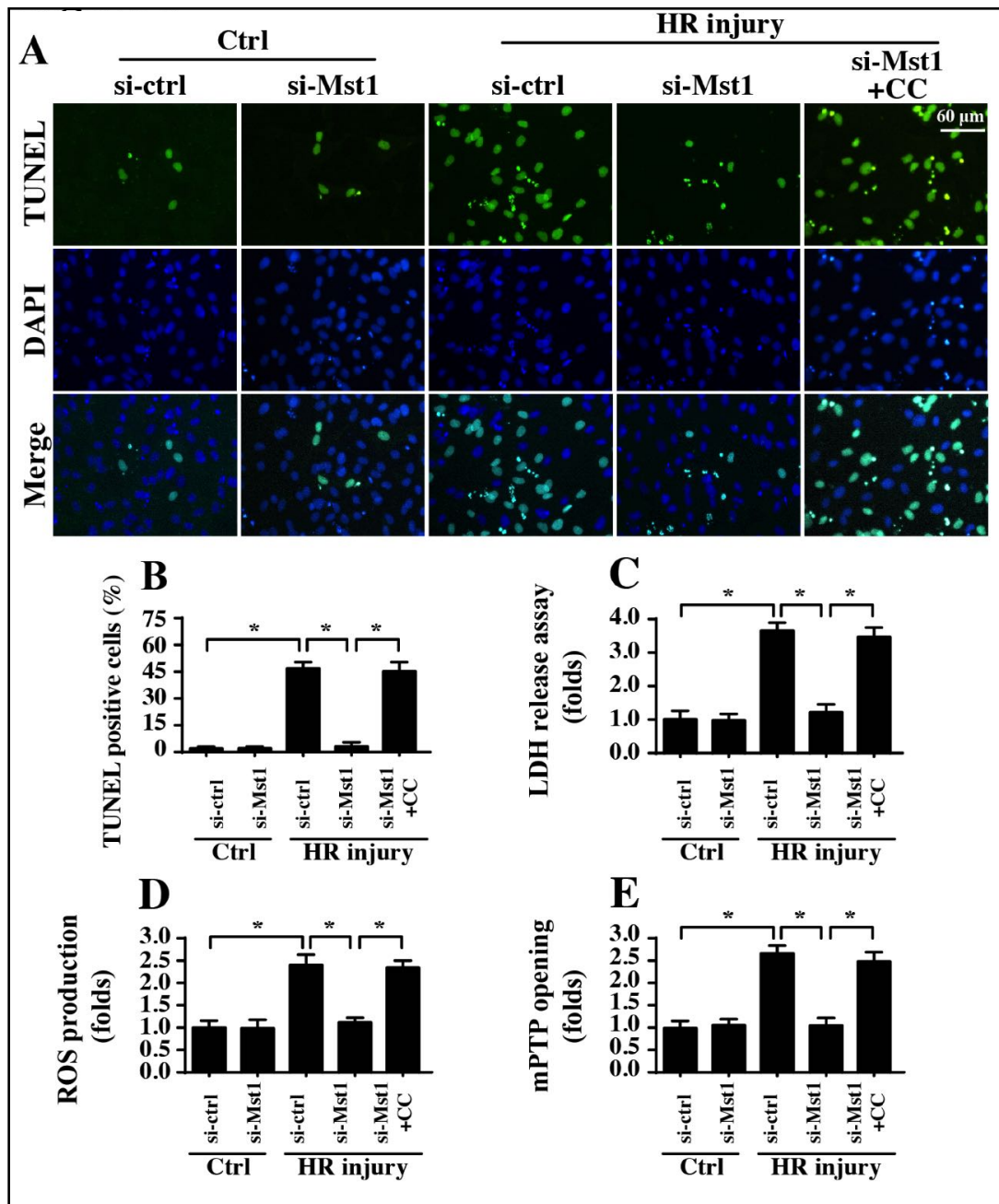


Fig. 6. AMPK-YAP pathways also participate into kidney cell death and mitochondrial damage in an I/R setting. A-B. TUNEL assay was performed to observe cell death, and the number of TUNEL-positive cells was monitored. Mst1 siRNA was transfected into the cells to inhibit Mst1 expression. Compound C (CC) was used to inhibit the AMPK-YAP pathways. C. LDH release assay for cell death in response to Mst1 deletion and AMPK inhibition. D. Cellular ROS production was measured via a DHE probe and was analyzed via flow cytometry. Mst1 siRNA was transfected into the cells to inhibit Mst1 expression. CC was used to inhibit the AMPK-YAP pathways. E. The ratio of mPTP opening was evaluated. *P<0.05.

reversed the communication between mitochondria and lysosomes; this effect was strongly negated by OPA1 siRNA (Fig. 5G-H). Overall, our data suggest that OPA1-related mitophagy is regulated by Mst1 via the AMPK-YAP cascade.

AMPK-YAP signaling pathway is also implicated in I/R-mediated mitochondrial apoptosis

Subsequently, we evaluated the role of the AMPK-YAP cascade in mitochondrial dysfunction and cell death under HR injury. Compared to the control group, HR increased the number of TUNEL-positive cells (Fig. 6A-B). However, HR-mediated cell apoptosis was inhibited by Mst1 deletion via activation of the AMPK-YAP signaling pathways (Fig. 6A-B). Similarly, the LDH release assay also illustrated that HR-evoked cell death could be mostly reversed by Mst1 deletion, and this effect was dependent on the AMPK-YAP cascade (Fig. 6C).

With respect to mitochondrial dysfunction, mitochondrial ROS was evaluated again, and the results indicated that HR-produced ROS could be reduced by Mst1 deletion (Fig. 6D), and this protective effect was achieved via activation of the AMPK-YAP cascade. Moreover, the mPTP opening rate was augmented by HR injury and was reversed to near-normal levels with Mst1 deletion (Fig. 6E). However, inhibition of the AMPK-YAP cascade, the inhibitory action of Mst1 deficiency on mPTP opening was abolished (Fig. 6E). Collectively, these results suggest that the AMPK-YAP cascade is also involved in Mst1-modulated renal cell death and mitochondrial dysfunction under HR injury.

Discussion

Revascularization is the standard treatment for ischemic kidney. However, reperfusion therapy also causes additional damage to the kidney tissue [47], which is defined as I/R injury in clinical practice [48]. In the present study, we explored the etiology of renal IR injury and found that the pathogenesis of kidney reperfusion damage was closely associated with Mst1 upregulation. Genetic ablation of Mst1 protected the kidney against I/R injury by regulating mitochondrial homeostasis. At the molecular level, inhibition of Mst1 reduced mitochondrial dysfunction and closed mitochondrial apoptosis in cell by recalling protective mitophagy. Increased mitophagy repressed HR-mediated cellular oxidative stress, ensured ATP supply, and blocked caspase-9 activation. Further, we demonstrated that Mst1 regulated mitophagy via OPA1, a mitophagic receptor. Loss of OPA1 abrogated the protective influence of Mst1 deletion on mitochondrial function. To this end, we demonstrated that OPA1-related mitophagy was primarily regulated by the AMPK-YAP signaling pathway. Blockade of the AMPK-YAP-OPA1 pathway disturbed Mst1-modified mitophagy and caused mitochondrial apoptosis in cell under IR injury.

The mitochondrial mass is rich in kidney cells. Additionally, the kidney has high mitochondrial oxidative metabolism and is exquisitely sensitive to hypoxic injury [49]. The function of renal tubular epithelial cells is primarily modulated by mitochondrial metabolism, making them more vulnerability to mitochondrial damage [50]. Accumulative evidence has established the critical role of mitochondrial injury in renal I/R injury. For example, elevated mitochondrial oxidative stress and deteriorated mitochondrial enzyme activation have been noted in the reperfused kidney [51]. In addition, inhibition of mitochondrial permeability transition pore opening via CsA has been proven to be beneficial for kidneys in the context of I/R injury [52]. Moreover, mitochondrial apoptosis has been acknowledged as the primary reason for reperfusion-mediated renal tubular epithelial cell apoptosis [53]. In addition, mitochondrial DNA damage [54], mitochondrial biosynthesis disorder [55], and mitophagy delay [56] have been found to be implicated in mitochondrial dysfunction and renal damage exerted by I/R injury. In the present study, we also found that mitochondria were the potential target of the renal I/R injury. Mitochondrial damage, such as mitochondrial potential reduction, ROS overproduction, energy undersupply, pro-apoptotic factor leakage, and caspase-9 activation, was fine-tuned by I/R injury. In addition, we illustrated that mitochondrial damage was attributable to mitophagy inhibition. Activation of mitophagy

blocked caspase-3 activation and attenuated reperfusion-mediated death in renal tubular epithelial cells. This finding is similar to that in previous reports demonstrating mitophagy is protective for the reperfused kidney [57, 58]. Therefore, this evidence firmly establishes the central role of mitochondria and the subsequent mitochondrial damage that amplifies the damage signal for the reperfused kidney.

Mst1, the downstream effector of the Hippo signalling pathway, is originally identified as the apoptotic trigger in several diseases such as post-infarction cardiac remodelling [59], breast cancer [60], acute brain injury [61] and liver fibrosis [62]. Notably, the action of Mst1 in kidney damage has not yet been explained. Accordingly, this is the first detailed investigation to uncover the causal relationship between Mst1 activation and acute renal damage. We confirmed that Mst1 repressed defensive mitophagy, as mitochondria were unable to repair themselves in a timely manner. Reactivation of mitophagy via depletion of Mst1 sustained cellular energy, repressed oxidative stress, and blocked mitochondrial apoptosis. This study is the first investigation to provide a piece of evidence for the inhibitory effect of Mst1 on mitophagy in the setting of renal I/R injury, suggesting that the strategies to reverse mitophagic activity at the stage of reperfusion would confer a prosurvival advantage for the kidney [63-65].

Further, we demonstrated that Mst1 regulated mitophagy via OPA1. Actually, several mitophagic receptors have been tested. For example, FUNDC1, the mitochondrial outer membrane proteins, has been acknowledged as the guard of heart function in the setting of acute IR injury [66]. In addition, Bnip3, another mitochondrial receptor, exerts beneficial effects on high-fat-treated livers [67]. In the present study, we explored the role of OPA1 in renal I/R injury. OPA1, the mitochondrial outer membrane GTPase, plays a key role in initiating mitophagy in pancreatic cancer, hepatic IR injury, Alzheimer's disease, and gastric cancer [68]. In agreement with a previous study, OPA1 activated mitophagy and subsequently degraded the damaged mitochondria, interrupting the mitochondrial damage signalling. Notably, whether Mst1 could modulate mitophagy via other receptors in renal I/R injury is far from clear. More studies are required to explore this.

Conclusion

Our results implicate Mst1 upregulation as a critical step in initiating renal I/R injury. Increased Mst1 blocks the AMPK-YAP pathway and thus diminishes OPA1 expression, repressing mitophagy and consequently activating mitochondrial apoptosis in reperfused kidneys. Thus, our findings reveal a novel molecular mechanism for the development of renal IR injury and suggest the regulatory importance of Mst1 and OPA1-mediated mitophagy in preserving kidney mitochondrial homeostasis.

Disclosure Statement

The authors declared that they have no conflicts of interest.

References

- 1 Nishikawa H, Taniguchi Y, Matsumoto T, Arima N, Masaki M, Shimamura Y, Inoue K, Horino T, Fujimoto S, Ohko K, Komatsu T, Udaka K, Sano S, Terada Y: Knockout of the interleukin-36 receptor protects against renal ischemia-reperfusion injury by reduction of proinflammatory cytokines. *Kidney Int* 2018;93:599-614.
- 2 Micanovic R, Khan S, Janosevic D, Lee ME, Hato T, Srour EF, Winfree S, Ghosh J, Tong Y, Rice SE, Dagher PC, Wu XR, El-Achkar TM: Tamm-Horsfall Protein Regulates Mononuclear Phagocytes in the Kidney. *J Am Soc Nephrol* 2018;29:841-856.

- 3 Liu L, Li H, Cui Y, Li R, Meng F, Ye Z, Zhang X: Calcium Channel Opening Rather than the Release of ATP Causes the Apoptosis of Osteoblasts Induced by Overloaded Mechanical Stimulation. *Cell Physiol Biochem* 2017;42:441-454.
- 4 Liu F, Ni W, Zhang J, Wang G, Li F, Ren W: Administration of Curcumin Protects Kidney Tubules Against Renal Ischemia-Reperfusion Injury (RIRI) by Modulating Nitric Oxide (NO) Signaling Pathway. *Cell Physiol Biochem* 2017;44:401-411.
- 5 Ren XS, Tong Y, Ling L, Chen D, Sun HJ, Zhou H, Qi XH, Chen Q, Li YH, Kang YM, Zhu GQ: NLRP3 Gene Deletion Attenuates Angiotensin II-Induced Phenotypic Transformation of Vascular Smooth Muscle Cells and Vascular Remodeling. *Cell Physiol Biochem* 2017;44:2269-2280.
- 6 Wei L, Zhang X, Ye Q, Yang Y, Chen X: The transfection of A20 gene prevents kidney from ischemia reperfusion injury in rats. *Mol Med Rep* 2017;16:1486-1492.
- 7 Zhou H, Zhu P, Wang J, Zhu H, Ren J, Chen Y: Pathogenesis of cardiac ischemia reperfusion injury is associated with CK2alpha-disturbed mitochondrial homeostasis via suppression of FUNDC1-related mitophagy. *Cell Death Differ* 2018;25:1080-1093.
- 8 Zhou H, Wang J, Zhu P, Hu S, Ren J: Ripk3 regulates cardiac microvascular reperfusion injury: The role of IP3R-dependent calcium overload, XO-mediated oxidative stress and F-actin/filopodia-based cellular migration. *Cell Signal* 2018;45:12-22.
- 9 Zhou H, Shi C, Hu S, Zhu H, Ren J, Chen Y: BI1 is associated with microvascular protection in cardiac ischemia reperfusion injury via repressing Syk-Nox2-Drp1-mitochondrial fission pathways. *Angiogenesis* 2018;21:599-615.
- 10 Zhou H, Wang J, Zhu P, Zhu H, Toan S, Hu S, Ren J, Chen Y: NR4A1 aggravates the cardiac microvascular ischemia reperfusion injury through suppressing FUNDC1-mediated mitophagy and promoting Mff-required mitochondrial fission by CK2alpha. *Basic Res Cardiol* 2018;113:23.
- 11 Zhu H, Jin Q, Li Y, Ma Q, Wang J, Li D, Zhou H, Chen Y: Melatonin protected cardiac microvascular endothelial cells against oxidative stress injury via suppression of IP3R-[Ca(2+)]c/VDAC-[Ca(2+)]m axis by activation of MAPK/ERK signaling pathway. *Cell Stress Chaperones* 2018;23:101-113.
- 12 Zhu P, Hu S, Jin Q, Li D, Tian F, Toan S, Li Y, Zhou H, Chen Y: Ripk3 promotes ER stress-induced necroptosis in cardiac IR injury: A mechanism involving calcium overload/XO/ROS/mPTP pathway. *Redox Biol* 2018;16:157-168.
- 13 Zhou H, Li D, Zhu P, Ma Q, Toan S, Wang J, Hu S, Chen Y, Zhang Y: Inhibitory effect of melatonin on necroptosis via repressing the Ripk3-PGAM5-CypD-mPTP pathway attenuates cardiac microvascular ischemia-reperfusion injury. *J Pineal Res* 2018;65:e12503.
- 14 Jin Q, Li R, Hu N, Xin T, Zhu P, Hu S, Ma S, Zhu H, Ren J, Zhou H: DUSP1 alleviates cardiac ischemia/reperfusion injury by suppressing the Mff-required mitochondrial fission and Bnip3-related mitophagy via the JNK pathways. *Redox Biol* 2018;14:576-587.
- 15 Zhou H, Zhu P, Guo J, Hu N, Wang S, Li D, Hu S, Ren J, Cao F, Chen Y: Ripk3 induces mitochondrial apoptosis via inhibition of FUNDC1 mitophagy in cardiac IR injury. *Redox Biol* 2017;13:498-507.
- 16 Zhou H, Zhang Y, Hu S, Shi C, Zhu P, Ma Q, Jin Q, Cao F, Tian F, Chen Y: Melatonin protects cardiac microvasculature against ischemia/reperfusion injury via suppression of mitochondrial fission-VDAC1-HK2-mPTP-mitophagy axis. *J Pineal Res* 2017;63:e12413.
- 17 Fuhrmann DC, Brune B: Mitochondrial composition and function under the control of hypoxia. *Redox Biol* 2017;12:208-215.
- 18 Zhou H, Wang S, Zhu P, Hu S, Chen Y, Ren J: Empagliflozin rescues diabetic myocardial microvascular injury via AMPK-mediated inhibition of mitochondrial fission. *Redox Biol* 2018;15:335-346.
- 19 Zhou H, Hu S, Jin Q, Shi C, Zhang Y, Zhu P, Ma Q, Tian F, Chen Y: Mff-Dependent Mitochondrial Fission Contributes to the Pathogenesis of Cardiac Microvasculature Ischemia/Reperfusion Injury via Induction of mROS-Mediated Cardiolipin Oxidation and HK2/VDAC1 Disassociation-Involved mPTP Opening. *J Am Heart Assoc* 2017;6: e005328.
- 20 Li S, Xu S, Roelofs BA, Boyman L, Lederer WJ, Sesaki H, Karbowski M: Transient assembly of F-actin on the outer mitochondrial membrane contributes to mitochondrial fission. *J Cell Biol* 2015;208:109-123.
- 21 Shi C, Cai Y, Li Y, Li Y, Hu N, Ma S, Hu S, Zhu P, Wang W, Zhou H: Yap promotes hepatocellular carcinoma metastasis and mobilization via governing cofilin/F-actin/lamellipodium axis by regulation of JNK/Bnip3/SERCA/CaMKII pathways. *Redox Biol* 2018;14:59-71.

- 22 Zhao Q, Ye M, Yang W, Wang M, Li M, Gu C, Zhao L, Zhang Z, Han W, Fan W, Meng Y: Effect of Mst1 on Endometriosis Apoptosis and Migration: Role of Drp1-Related Mitochondrial Fission and Parkin-Required Mitophagy. *Cell Physiol Biochem* 2018;45:1172-1190.
- 23 Sun Y, Li Q, Zhang J, Chen Z, He Q, Liu X, Zhao N, Yin A, Huang H, He M, Cao L, Wang L: Autophagy regulatory molecule, TMEM74, interacts with BIK and inhibits BIK-induced apoptosis. *Cell Signal* 2017;36:34-41.
- 24 Liu D, Zeng X, Li X, Mehta JL, Wang X: Role of NLRP3 inflammasome in the pathogenesis of cardiovascular diseases. *Basic Res Cardiol* 2017;113:5.
- 25 Li J, Chen L, Xiong Y, Zheng X, Xie Q, Zhou Q, Shi L, Wu C, Jiang J, Wang H: Knockdown of PD-L1 in Human Gastric Cancer Cells Inhibits Tumor Progression and Improves the Cytotoxic Sensitivity to CIK Therapy. *Cell Physiol Biochem* 2017;41:907-920.
- 26 Ligeza J, Marona P, Gach N, Lipert B, Miekus K, Wilk W, Jaszczynski J, Stelmach A, Loboda A, Dulak J, Branicki W, Rys J, Jura J: MCP1P1 contributes to clear cell renal cell carcinomas development. *Angiogenesis* 2017;20:325-340.
- 27 Ronchi C, Torre E, Rizzetto R, Bernardi J, Rocchetti M, Zaza A: Late sodium current and intracellular ionic homeostasis in acute ischemia. *Basic Res Cardiol* 2017;112:12.
- 28 Lin S, Hoffmann K, Gao C, Petrulionis M, Herr I, Schemmer P: Melatonin promotes sorafenib-induced apoptosis through synergistic activation of JNK/c-jun pathway in human hepatocellular carcinoma. *J Pineal Res* 2017;62:e12398.
- 29 Shin D, Kim EH, Lee J, Roh JL: RITA plus 3-MA overcomes chemoresistance of head and neck cancer cells via dual inhibition of autophagy and antioxidant systems. *Redox Biol* 2017;13:219-227.
- 30 Costa F, Yamaki VN, Teixeira RKC, Feijo DH, Valente AL, Carvalho LTF, Yasojima EY, Brito MVH: Preconditioning combined with postconditioning on kidney ischemia and reperfusion. *Acta Cir Bras* 2017;32:599-606.
- 31 Wang K, Gan TY, Li N, Liu CY, Zhou LY, Gao JN, Chen C, Yan KW, Ponnusamy M, Zhang YH, Li PF: Circular RNA mediates cardiomyocyte death via miRNA-dependent upregulation of MTP18 expression. *Cell Death Differ* 2017;24:1111-1120.
- 32 Zhang Y, Zhou H, Wu W, Shi C, Hu S, Yin T, Ma Q, Han T, Zhang Y, Tian F, Chen Y: Liraglutide protects cardiac microvascular endothelial cells against hypoxia/reoxygenation injury through the suppression of the SR-Ca(2+)-XO-ROS axis via activation of the GLP-1R/PI3K/Akt/survivin pathways. *Free Radic Biol Med* 2016;95:278-292.
- 33 Zhang W, Tao A, Lan T, Cepinskas G, Kao R, Martin CM, Rui T: Carbon monoxide releasing molecule-3 improves myocardial function in mice with sepsis by inhibiting NLRP3 inflammasome activation in cardiac fibroblasts. *Basic Res Cardiol* 2017;112:16.
- 34 Das N, Mandala A, Naaz S, Giri S, Jain M, Bandyopadhyay D, Reiter RJ, Roy SS: Melatonin protects against lipid-induced mitochondrial dysfunction in hepatocytes and inhibits stellate cell activation during hepatic fibrosis in mice. *J Pineal Res* 2017;62:e12404.
- 35 Torres-Estay V, Carreno DV, Fuenzalida P, Watts A, San Francisco IF, Montecinos VP, Sotomayor PC, Ebo J, Smith GJ, Godoy AS: Androgens modulate male-derived endothelial cell homeostasis using androgen receptor-dependent and receptor-independent mechanisms. *Angiogenesis* 2017;20:25-38.
- 36 Feng D, Wang B, Wang L, Abraham N, Tao K, Huang L, Shi W, Dong Y, Qu Y: Pre-ischemia melatonin treatment alleviated acute neuronal injury after ischemic stroke by inhibiting endoplasmic reticulum stress-dependent autophagy via PERK and IRE1 signalings. *J Pineal Res* 2017;62:e12395.
- 37 Zong C, Qin D, Yu C, Gao P, Chen J, Lu S, Zhang Y, Liu Y, Yang Y, Pu Z, Li X, Fu Y, Guan Q, Wang X: The stress-response molecule NR4A1 resists ROS-induced pancreatic beta-cells apoptosis via WT1. *Cell Signal* 2017;35:129-139.
- 38 Zhang R, Sun Y, Liu Z, Jin W, Sun Y: Effects of melatonin on seedling growth, mineral nutrition, and nitrogen metabolism in cucumber under nitrate stress. *J Pineal Res* 2017;62:e12403.
- 39 Zhou H, Li D, Zhu P, Hu S, Hu N, Ma S, Zhang Y, Han T, Ren J, Cao F, Chen Y: Melatonin suppresses platelet activation and function against cardiac ischemia/reperfusion injury via PPARgamma/FUNDC1/mitophagy pathways. *J Pineal Res* 2017;63:e12438.
- 40 Jovancevic N, Dendorfer A, Matzkies M, Kovarova M, Heckmann JC, Osterloh M, Boehm M, Weber L, Nguemo F, Semmler J, Hescheler J, Milting H, Schleicher E, Gelis L, Hatt H: Medium-chain fatty acids modulate myocardial function via a cardiac odorant receptor. *Basic Res Cardiol* 2017;112:13.

- 41 Fan T, Pi H, Li M, Ren Z, He Z, Zhu F, Tian L, Tu M, Xie J, Liu M, Li Y, Tan M, Li G, Qing W, Reiter RJ, Yu Z, Wu H, Zhou Z: Inhibiting MT2-TFE3-dependent autophagy enhances melatonin-induced apoptosis in tongue squamous cell carcinoma. *J Pineal Res* 2018;64:e12457.
- 42 Dong X, Fu J, Yin X, Qu C, Yang C, He H, Ni J: Induction of Apoptosis in HepaRG Cell Line by Aloe-Emodin through Generation of Reactive Oxygen Species and the Mitochondrial Pathway. *Cell Physiol Biochem* 2017;42:685-696.
- 43 Lassen TR, Nielsen JM, Johnsen J, Ringgaard S, Botker HE, Kristiansen SB: Effect of paroxetine on left ventricular remodeling in an *in vivo* rat model of myocardial infarction. *Basic Res Cardiol* 2017;112:26.
- 44 Zhou H, Ma Q, Zhu P, Ren J, Reiter RJ, Chen Y: Protective role of melatonin in cardiac ischemia-reperfusion injury: From pathogenesis to targeted therapy. *J Pineal Res* 2018;64:e12471.
- 45 Rossello X, Riquelme JA, He Z, Taferner S, Vanhaesebroeck B, Davidson SM, Yellon DM: The role of PI3Kalpha isoform in cardioprotection. *Basic Res Cardiol* 2017;112:66.
- 46 Liu Z, Gan L, Luo D, Sun C: Melatonin promotes circadian rhythm-induced proliferation through Clock/histone deacetylase 3/c-Myc interaction in mouse adipose tissue. *J Pineal Res* 2017;62:e12383.
- 47 Zhou J, Zhong J, Lin S, Huang Z, Chen H, Tang S, Yang C, Fan Y: Inhibition of PTEN Activity Aggravates Post Renal Fibrosis in Mice with Ischemia Reperfusion-Induced Acute Kidney Injury. *Cell Physiol Biochem* 2017;43:1841-1854.
- 48 Merjaneh M, Langlois A, Larochelle S, Cloutier CB, Ricard-Blum S, Moulin VJ: Pro-angiogenic capacities of microvesicles produced by skin wound myofibroblasts. *Angiogenesis* 2017;20:385-398.
- 49 Tallman KA, Kim HH, Korade Z, Genaro-Mattos TC, Wages PA, Liu W, Porter NA: Probes for protein adduction in cholesterol biosynthesis disorders: Alkynyl lanosterol as a viable sterol precursor. *Redox Biol* 2017;12:182-190.
- 50 Shen YQ, Guerra-Librero A, Fernandez-Gil BI, Florido J, Garcia-Lopez S, Martinez-Ruiz L, Mendivil-Perez M, Soto-Mercado V, Acuna-Castroviejo D, Ortega-Arellano H, Carriel V, Diaz-Casado ME, Reiter RJ, Rusanova I, Nieto A, Lopez LC, Escames G: Combination of melatonin and rapamycin for head and neck cancer therapy: Suppression of AKT/mTOR pathway activation, and activation of mitophagy and apoptosis via mitochondrial function regulation. *J Pineal Res* 2018;64:12461.
- 51 Schock SN, Chandra NV, Sun Y, Irie T, Kitagawa Y, Gotoh B, Coscoy L, Winoto A: Induction of necroptotic cell death by viral activation of the RIG-I or STING pathway. *Cell Death Differ* 2017;24:615-625.
- 52 Rossello X, Yellon DM: The RISK pathway and beyond. *Basic Res Cardiol* 2017;113:2.
- 53 Tan XH, Zheng XM, Yu LX, He J, Zhu HM, Ge XP, Ren XL, Ye FQ, Bellusci S, Xiao J, Li XK, Zhang JS: Fibroblast growth factor 2 protects against renal ischaemia/reperfusion injury by attenuating mitochondrial damage and proinflammatory signalling. *J Cell Mol Med* 2017;21:2909-2925.
- 54 Zhou H, Yue Y, Wang J, Ma Q, Chen Y: Melatonin therapy for diabetic cardiomyopathy: A mechanism involving Syk-mitochondrial complex I-SERCA pathway. *Cell Signal* 2018;47:88-100.
- 55 Li R, Xin T, Li D, Wang C, Zhu H, Zhou H: Therapeutic effect of Sirtuin 3 on ameliorating nonalcoholic fatty liver disease: The role of the ERK-CREB pathway and Bnip3-mediated mitophagy. *Redox Biol* 2018;18:229-243.
- 56 Zhou H, Wang S, Hu S, Chen Y, Ren J: ER-Mitochondria Microdomains in Cardiac Ischemia-Reperfusion Injury: A Fresh Perspective. *Front Physiol* 2018;9:755.
- 57 Nauta TD, van den Broek M, Gibbs S, van der Pouw-Kraan TC, Oudejans CB, van Hinsbergh VW, Koolwijk P: Identification of HIF-2alpha-regulated genes that play a role in human microvascular endothelial sprouting during prolonged hypoxia *in vitro*. *Angiogenesis* 2017;20:39-54.
- 58 Tobisawa T, Yano T, Tanno M, Miki T, Kuno A, Kimura Y, Ishikawa S, Kouzu H, Nishizawa K, Yoshida H, Miura T: Insufficient activation of Akt upon reperfusion because of its novel modification by reduced PP2A-B55alpha contributes to enlargement of infarct size by chronic kidney disease. *Basic Res Cardiol* 2017;112:31.
- 59 Yu S, Wang X, Geng P, Tang X, Xiang L, Lu X, Li J, Ruan Z, Chen J, Xie G, Wang Z, Ou J, Peng Y, Luo X, Zhang X, Dong Y, Pang X, Miao H, Chen H, Liang H: Melatonin regulates PARP1 to control the senescence-associated secretory phenotype (SASP) in human fetal lung fibroblast cells. *J Pineal Res* 2017;63:e12405.
- 60 Xu J, Wu Y, Lu G, Xie S, Ma Z, Chen Z, Shen HM, Xia D: Importance of ROS-mediated autophagy in determining apoptotic cell death induced by physapubescin B. *Redox Biol* 2017;12:198-207.
- 61 Nunez-Gomez E, Pericacho M, Ollauri-Ibanez C, Bernabeu C, Lopez-Novoa JM: The role of endoglin in post-ischemic revascularization. *Angiogenesis* 2017;20:1-24.

- 62 Tomczyk M, Kraszewska I, Szade K, Bukowska-Strakova K, Meloni M, Jozkowicz A, Dulak J, Jazwa A: Splenic Ly6C(hi) monocytes contribute to adverse late post-ischemic left ventricular remodeling in heme oxygenase-1 deficient mice. *Basic Res Cardiol* 2017;112:39.
- 63 Vargas LA, Velasquez FC, Alvarez BV: Compensatory role of the NBCn1 sodium/bicarbonate cotransporter on Ca(2+)-induced mitochondrial swelling in hypertrophic hearts. *Basic Res Cardiol* 2017;112:14.
- 64 Sarkar C, Ganju RK, Pompili VJ, Chakroborty D: Enhanced peripheral dopamine impairs post-ischemic healing by suppressing angiotensin receptor type 1 expression in endothelial cells and inhibiting angiogenesis. *Angiogenesis* 2017;20:97-107.
- 65 Van Nostrand JL, Bowen ME, Vogel H, Barna M, Attardi LD: The p53 family members have distinct roles during mammalian embryonic development. *Cell Death Differ* 2017;24:575-579.
- 66 Yang G, Zhang X, Weng X, Liang P, Dai X, Zeng S, Xu H, Huan H, Fang M, Li Y, Xu D, Xu Y: SUV39H1 mediated SIRT1 trans-repression contributes to cardiac ischemia-reperfusion injury. *Basic Res Cardiol* 2017;112:22.
- 67 Yang X, Xu Y, Wang T, Shu D, Guo P, Miskimins K, Qian SY: Inhibition of cancer migration and invasion by knocking down delta-5-desaturase in COX-2 overexpressed cancer cells. *Redox Biol* 2017;11:653-662.
- 68 Thirusangu P, Vigneshwaran V, Prashanth T, Vijay Avin BR, Malojirao VH, Rakesh H, Khanum SA, Mahmood R, Prabhakar BT: BP-1T, an antiangiogenic benzophenone-thiazole pharmacophore, counteracts HIF-1 signalling through p53/MDM2-mediated HIF-1alpha proteasomal degradation. *Angiogenesis* 2017;20:55-71.